

# Voyage to the Bottom of the Puerto Rico Trench: Tales from a free fall current meter

Wilford Schmidt  
Department of Marine Sciences  
University of Puerto Rico, Mayagüez  
Mayagüez, Puerto Rico, USA

Eric Siegel  
NortekUSA  
222 Severn Avenue  
Annapolis, USA

**Abstract**—Near-bottom (~2 m) current velocities in the Puerto Rico Trench (~8350 m depth) were measured at 1 Hz for 75 min by a Nortek Deep Water Aquadopp acoustic-Doppler current meter at 19.75° N, 66.40° W, via untethered free descent/ascent vehicle. The April 2008 deployment also recorded 3-axis velocity, temperature, pressure, and instrument heading, pitch, roll, and signal-strength during the 153 min free descent, and while on bottom. Signal strength was above the noise floor for the entire data set, and SNR and velocity standard deviation were within known acceptable bounds above 7000 m. Instrument heading showed a continuous anti-clockwise rotation during descent. Doppler vertical velocity during descent is compared to the pressure time derivative. Integration of horizontal velocity during descent suggests a lateral displacement of less than 30 m over the 8.35 km free-fall. Measurements made at impact indicate full functionality of the instrument at depth. Maximum horizontal velocities while on-bottom varied between 1 cm/s and 5 cm/s and were directed roughly along trench axis westward.

## I. INTRODUCTION

Physical oceanographic measurements in and around Puerto Rico have a long history, in part because of its U.S. commonwealth status and in part due to the previous Navy presence. As with most of the world's oceans, the deep abyssal and hadal waters have seen the least sampling. In fact, current velocity and water property measurements spanning the water column over the world's deep oceanic trenches (>8 km) are exceedingly rare [1]. This stems from the fact that steel wire typically used for hydrographic casts is not suitable for use below about 7 km due to breaking strength limitations. Sporadic hadal measurements in Pacific basin trenches appear in the literature [1, 2, 3, 4], although the direct current measurements in these references were made with rotor-type current meters, not the acoustic Doppler current meter style reported here. Similar measurements in the Puerto Rico Trench (PRT) are even rarer. Recent reports [5, 6] were limited to maximum sampling depths of 6000 m. In the absence of current meter and CTD data, flows are assumed to be small or zero; therefore highlighting the need and rationale for this work.

In April 2008, a Nortek Deep Water Aquadopp current meter was deployed in the PRT to approximately 8350 m at 19.75° N, 66.40° W, via untethered free-descent/ascent vehicle (Fig. 1). Free-vehicles operate under the principle that an untethered, negatively buoyant object will descend freely to the sea-bed, and will ascend freely back to the surface if made positively buoyant. The free-vehicle deployed here was developed as a partnership formed in 2006 between the University of Puerto Rico, Mayaguez Department of Marine Sciences (UPRM/DMS) and the University of California, San Diego Scripps Institution of Oceanography. The goal was to develop and deploy free-vehicles to explore the ultra-deep (>8 km) PRT, the deepest part of the Atlantic Ocean and the seventh deepest trench on Earth. This proof of concept project laid the groundwork for modern, low-cost, free-vehicle hadal exploration [7, 8].

## II. MATERIALS AND METHODS

The free-vehicle was deployed from the UPRM/DMS RV Pez Mar, a 16 m long research vessel. An external ballast of steel chain (36 kg, 19 l (5 gal bucket)) overcame the buoyant force of two 43 cm diameter glass spheres until being released by timer-activated burnwire (Fig. 2). The current meter employed was a 2 MHz Aquadopp Deep Water current meter provided by NortekUSA. The Deep Water Aquadopp current meter has a published depth rating of 6000 m. Despite gray literature reports to the contrary [9], when conceiving of this project, Nortek engineers were consulted regarding the design safety factor of this instrument and it was determined that the 1.5 safety factor reported supported a maximum deployment depth of about 9000 m. Based on this information, all parties agreed that a PRT deployment of 2 hours on bottom was feasible. Unfortunately, the free-vehicle never surfaced after deployment and was deemed lost after a 36 hour search.

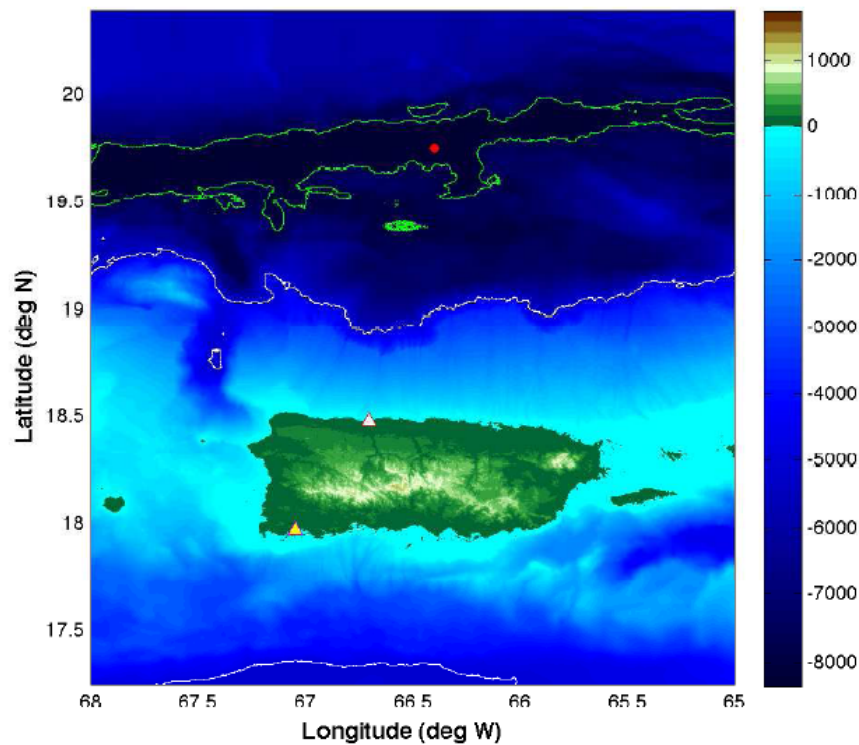


Fig.1 Study site. Triangles: UPRM DMS Marine Laboratories (yellow ) and Arecibo Harbor (white). Red point: 2008 deployment. Contours: -5000 m (white) and -8000 m (green). Bathymetry from USGS and NGDC.



Fig.2 (left) Free-vehicle assembly from Apr 2008 deployment showing flotation spheres (orange); and Nortek Aquadopp current meter, counter-balance, and frame (dark gray). Ballast was suspended below the current meter assembly by 2 m steel chain (not shown). (right) Close up of Aquadopp transducer head and free-vehicle burn wire. Steel chain suspends ballast below free-vehicle (not shown). An identical burn-wire assembly is found on the other side of the ADCM frame and functions as a secondary, 'fail-safe' ballast release.

Ten months later, an email titled "We found one of these" was received from the captain of the fishing boat Destiny. The entire free-vehicle had been found and recovered near 27° N, 71° W, or roughly 900 km east of Miami. After a finder's fee was negotiated with the fishing boat crew (\$100 and a case of beer), the Aquadopp was returned to NortekUSA, tested, and found to have some internal damage due to water. It was then sent to Nortek headquarters in Norway, where the memory chip was carefully removed from the corroded circuit board and its contents downloaded. Data had been logged for almost 4 hours, spanning the entire descent and including 75 minutes of on-bottom measurements. The time-series ended before the

scheduled ascent time, so it is not known when the free-vehicle began its return to the surface. It is postulated that one or probably both of the ballast release circuits malfunctioned, and the burn-wires became a long-lived galvanic releases. Future deployments will include galvanic releases of known duration.

The Aquadopp was configured with a 'mooring-style' transducer head optimized to measure horizontal currents with low standard deviation. The transducer head geometry had 2 acoustic beams directed horizontally (with 90° separation) and one acoustic beam directed at a 45° angle to the vertical (Fig. 2, right). The only information about the vertical component of the current is obtained from the single 45° beam.

A 1 Hz sample rate was chosen to optimize sampling from the free-vehicle. Since it was a possibility that the platform would tilt slightly and rotate during the free-descent, it was critical to measure the current velocity at the same time that other engineering data (e.g., heading, pitch, roll, and pressure) were recorded. Observe deviations from vertical during descent due to pitch and roll were small (mean 1.5° and 0.25°; std 0.3° and 0.25°, respectively). This was a result of the strong righting moment inherent in the free-vehicle design. A 'worst case scenario' horizontal displacement resulting from pitch and roll values during descent would be about 300 m.

However, since the free-vehicle rotated continuously during descent (shown below), the expected displacement would be much less. Since the Aquadopp requires scatter material in the water to reflect acoustic signals, a major concern in deep water environments is that limited scatter material will increase the velocity standard deviation (STD) and possibly bias the velocity data. In typical conditions with adequate scatters (i.e., good signal-to-noise ratio (SNR)), the predicted STD for 1 Hz data collected with this transducer head geometry is 2.3 cm/s for horizontal currents and 4.0 cm/s for vertical currents. The Aquadopp current meter has been demonstrated to work well, with no velocity bias, down to an SNR of about 6 [10]. There have been limited tests of the Aquadopp in water with SNR below 6.

### III. DISCUSSION

Water depth from pressure was 8535 m, significantly (2.4%) deeper than recent multibeam soundings from the same location of 8334 m [11 and U. ten Brink, personal communications]. It was determined that the pressure sensor in the Aquadopp is not compensated for changes in temperature, and this can account for up to 2% error in pressure at these depths.

To deal with this discrepancy, a correction, increasing linearly from 0% at the surface to 2% on bottom, was applied. Signal strength starts high (~80 counts) in the high-scatterer surface environment (Fig. 3), but below there decreases rapidly to about 40 counts (~5500 m), where it fairly constant until it begins to drop again below 7000 m. SNR is also high in the surface layer and drops to approximately 10 below 800 m. Below 3000 m, SNR falls again to just above 6 and remains roughly constant until 6200 m. Below 6200 m, SNR drops linearly with depth to about 2.

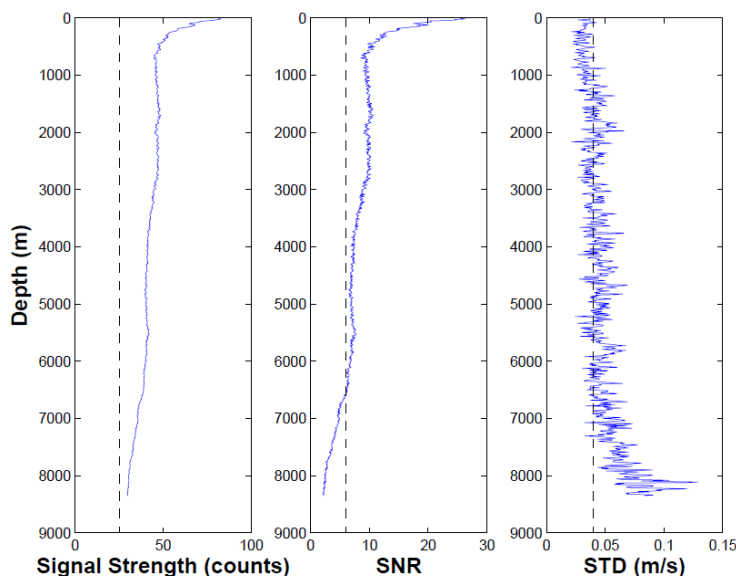


Fig.3 (left) Signal Strength vs. depth. The signal strength noise floor is indicated by dashed black line. (center) SNR vs. depth. The Aquadopp has been demonstrated to work well, with no velocity bias, down to an SNR of about 6, shown with black dashed line. Performance in SNR below 6 is unknown. (right) Vertical velocity standard deviation vs. depth. The expected standard deviation of 1 Hz data is 4.0 cm/s (black dashed line).

STD in the near-surface region with high SNR is about 3.0 cm/s, and in the region from 1000 m to 7000 m is near the predicted 4.0 cm/s. STD continues to increase below 7000 m where the SNR falls below 5. Maximum STD is approximately 10 cm/s, occurring on bottom where the SNR is at its lowest. This suggests Doppler measurements made during descent above 7000 m are well within acceptable SNR norms, whereas measurements during descent below 7000 m may suffer from low SNR.

Possible errors or biases of a free-falling current meter associated with high STD can be assessed by comparing the Doppler vertical velocity ( $W$ ) and the free-fall velocity estimated from the pressure time derivative ( $dP/dt$ ). First,  $W$  had to be corrected for significant pressure effects on sound speed present at hadal depths [12] (Fig. 4). The corrected quantities compare well, except for extended intervals where  $W$  is less than  $dP/dt$  (under-bias). This under-bias does not appear to be correlated with regions of low SNR or high STD. Rather, it appears concurrent to intervals of relatively low Doppler horizontal velocity ( $U$ ) (Fig. 5). The vertical velocity difference ( $W - dP/dt$ ), when compared with  $U$  (Fig. 6), shows systematic under-bias associated with regions of relatively low  $U$ .

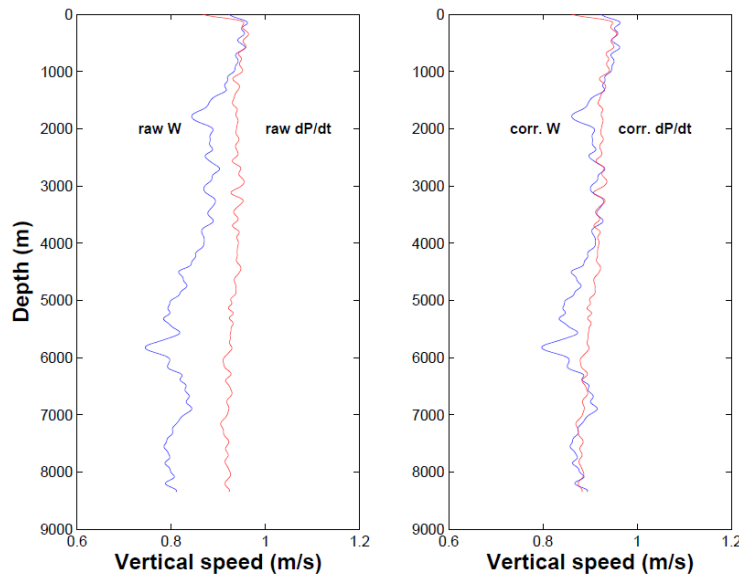


Fig.4 (left) Raw Doppler vertical velocity ( $W$ ) and pressure time derivative ( $dP/dt$ ) vs. depth. (right) Corrected  $W$  (after Morgan, 1993) and  $dP/dt$  (after UNESCO Eq. 25). All Doppler velocities are 120 s low-pass filtered. Subsequent figures reflect corrected values. The free fall speed of the platform was about 0.9 m/s. Doppler vertical velocities are under-biased with respect to the pressure time derivative between the depths of 1400 - 2750 m, 4000 - 6500 m, and 7300 - 8100 m.

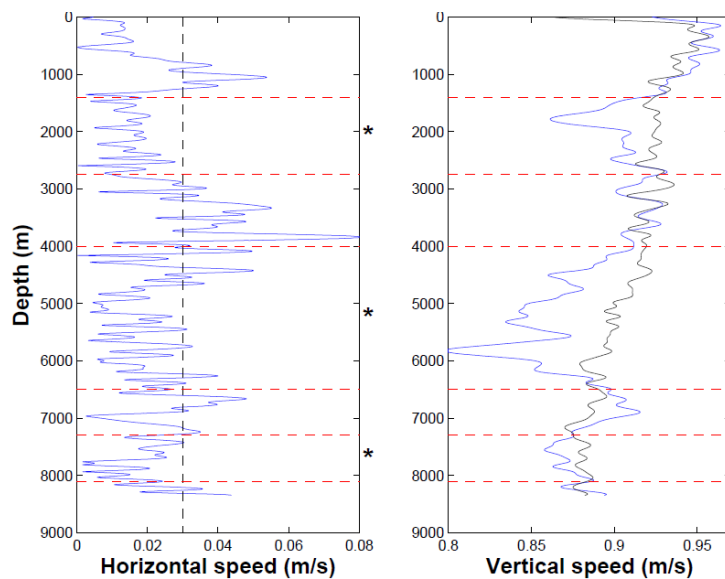


Fig.5 (left) Doppler horizontal velocity ( $U$ ) magnitude (speed, blue curve) vs. depth. (right)  $W$  magnitude (speed, blue curve) and  $dP/dt$  (black curve) vs. depth. Red dashed lines and asterisks roughly denote periods of vertical speed under-bias.

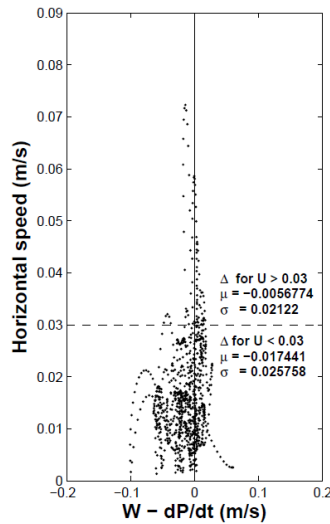


Fig.6 Scatter plot of U vs.  $W - dP/dt$ . Systematic velocity under-bias is observed when horizontal speed is below 0.03 m/s.

The cause of the under-biased  $W$  is not known for sure, but because it is linked to times of relatively low horizontal velocity, it is speculated also related to lower tilt of the entire free fall package. This suggests that the intervals of under-biased  $W$  are when the free-vehicle is descending very nearly vertically, and the zero bias  $W$  intervals are when there is oblique descent (i.e., descent with lateral displacement). A possible mechanism for this phenomenon is that during vertical descent, eddies shed by the ballast below the Aquadopp impinge on the measurement volume and contaminate the velocity measurements. During periods of slightly oblique descent, lateral displacement of the free-vehicle causes the eddies to 'miss' the measurement volume.

A map of the free-vehicle's horizontal displacement during descent can be created using the 2-axis horizontal velocity record and  $dP/dt$  (i.e., their integral with respect to time). However, one more question regarding  $U$  must be addressed. The direction is reported in a stationary frame and since the instrument is actually in motion, the direction must be rotated  $180^\circ$ . After this detail is addressed, the integration can be performed and the results, commonly known as a progressive vector diagram, presented (Fig 7). An irregular, spiraling trajectory is indicated with the bottom location  $<30$  m in the horizontal from the surface deployment. Much of the horizontal displacement is observed to occur between about 3000 m and 5000 m. The spiral pattern presumably represents the cork-screw motion of the free vehicle during descent. Accelerometer instrumentation and testing is planned to determine the general veracity of this finding. It is thought that the horizontal displacement (and dominant cyclonic rotation) is an artifact of free-vehicle geometry, rather than ambient currents (or Coriolis).

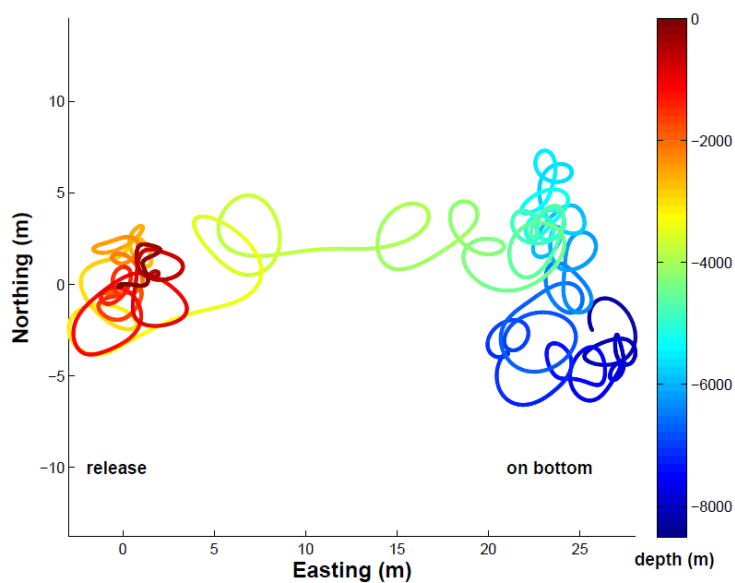


Fig.7 Horizontal velocity ( $U$ ) progressive vector diagram during descent. Surface release point and on bottom location are indicated by "release" and "on bottom", respectively.

Another assessment of the Aquadopp's performance is in the record just before and after reaching PRT bottom. Fig. 8 (a) shows the pressure record vs. time as the free-vehicle ballast impacts the bottom (IB) at almost 1 m/s, then stops. The instrument heading (Fig. 8 (b)) shows the rotation previously discussed until IB, after which a slight twisting on the 2 m chain linking ballast and free-vehicle can be discerned.

Unfiltered W (Fig. 8 (c)) agrees well with pressure. As the free-vehicle IB, W would be expected to decrease downward as inertia is dissipated in the 2 m distance above the ballast, then accelerate upward due to buoyancy until stopped by the ballast. The first two red points in Fig. 8 (c) appear to show this. Note that this will not be reflected in the pressure time series due to resolution limits. Low-passed horizontal velocities (U and V) (Fig. 8 (d)) exhibit the classic sine-cosine pattern associated with rotational motions and vary between about -0.05 m/s and 0.05 m/s until IB when they no longer oscillate and decrease in magnitude. The twisting observed in Fig. 8 (b) is not present in the filtered U and V.

Signal strength is a function of the scattering environment and is low before IB, but above the noise floor of 25 counts (black dashed line, Fig. 8 (e)). There is no change at IB, but after approximately 20 s, a slight decrease is noticed along with more variability. At about IB+35 s, higher signal strengths begin to be observed and greater variability. This is interpreted as sediment clouds raised by the ballast impact being advected into the sampling volume.

The 75 min on bottom time series of U magnitude and direction is shown in Fig. 9 (top and bottom, respectively). U magnitude varied between about 0.01 m/s and 0.05 m/s with an overall increasing trend, and was essentially directed along the PRT axis towards the west. A constant current of this magnitude would advect a water parcel along the PRT axis, from the eastern to western termini in approximately 0.5 yr.

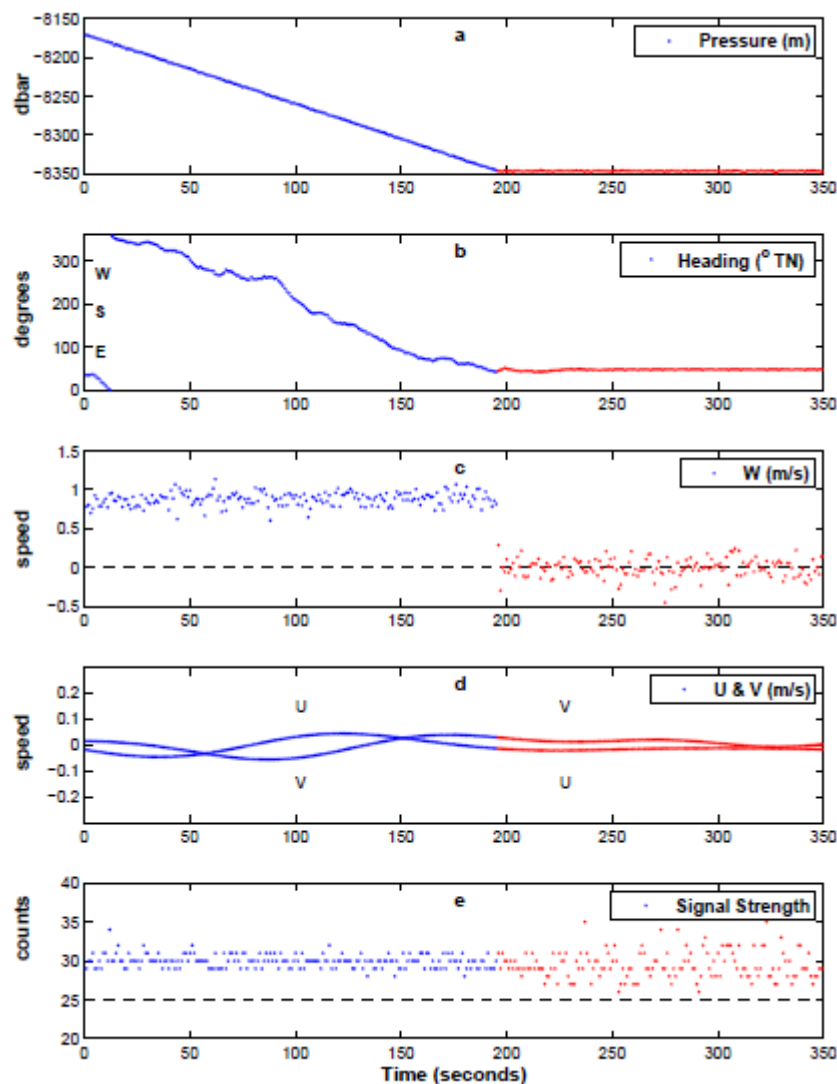


**Fig.8** Selected measurements at impact vs. time. (a) Pressure (b) Instrument heading. (c) Vertical speed. (d) Horizontal speeds (e) Signal strength. Blue curves and points denote measurements made prior to impact. Red curves and points denote measurements made after impact.

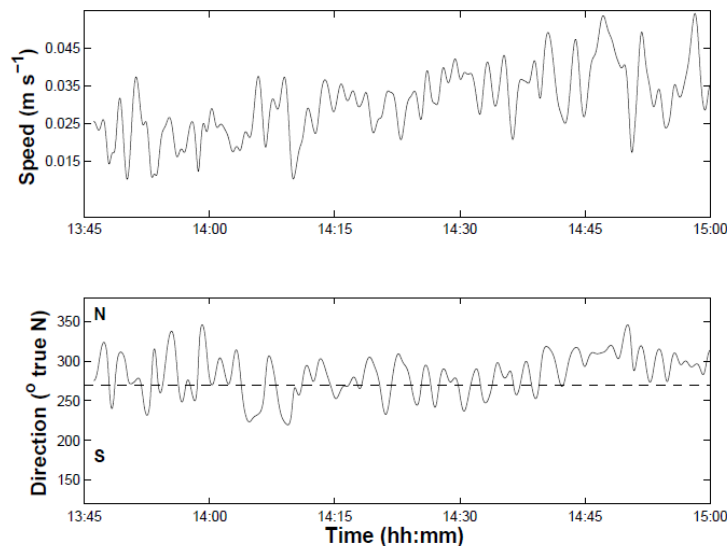


Fig.9 (top) On-bottom current speed. (bottom) On-bottom current direction. Black dashed line indicates westward direction.

#### IV. CONCLUSIONS

As expected, the low-scatterer environment below 6000 m proved challenging for acoustic-Doppler techniques. However, signal strength remained above minimum levels throughout the deployment and independent measurements such as  $dP/dt$  and instrument heading validate the data collected. W and U suggest a spiraling and remarkably direct descent to the PRT floor.

Measurements made at impact show that the ADCM was functioning normally at that time and the on-bottom time series indicates a 1 to 5 cm/s westward flow during its 75 min duration. Although short, this data set is important in several ways. Use of free-vehicle technology, especially in hadal work, is increasing and the engineering insights provided here will assist in future deployments. The on-bottom time series is the only dedicated hadal Doppler velocity measurement deployment known. It was also closer ( $< 3$  m) to the hadal ocean floor than any other current meter deployment, and had a much more rapid sample rate [1].

#### ACKNOWLEDGEMENTS

Support for this work and analysis was provided by National Science Foundation and the UPRM College of Arts and Sciences Seed Money Program. The authors would like to thank Trap Puckette, Doug Bartlett, Kevin Hardy, Roger Chastain, Emiley Eloë, Christine Shulse, and Atle Lohrmann for their contributions both on and off the water. The Scripps Institution of Oceanography Hydraulics Laboratory staff and the UPRM DMS Marine Section were also instrumental in the success of this project. Finally, special thanks to Captain Billy and the crew of the good ship Destiny, for keeping a sharp lookout.

#### REFERENCES

- [1] Taira, K., Kitagawa, S., Yamashiro T., and Yanagimoto, D. (2004). Deep and bottom currents in the Challenger Deep, Mariana Trench, measured with super-deep current meters. *J Oceanogr* 60: 919-926.
- [2] Mantyla, A., and Reid, J. (1978). Measurements of water characteristics at depth greater than 10 km in the Marianas Trench. *Deep-Sea Res* 25: 169-173.
- [3] Johnson, G. (1998). Deep water properties, velocities, and dynamics over ocean trenches. *J Mar Res* 56: 329-347.
- [4] Taira, K., Yanagimoto D., and Kitagawa, S. (2005). Deep CTD Casts in the Challenger Deep, Mariana Trench. *J Oceanogr* 61: 447-454.
- [5] Joyce T.M., Hernades-Guerra, A., and Smethie W.M. (2001). Zonal circulation in the NW Atlantic and Caribbean from a meridional World Ocean Circulation Experiment hydrographic section at 66 W. *J Geophys Res* 106: 22095-22113.
- [6] Steinfeldt, R., Rheim, M., and Walter, M. (2007). NADW transformation at the western boundary between 66 W/20N and 60 W/10 N. *Deep-Sea Res (I Oceanogr Res Pap)* 54: 835-855.
- [7] Eloë, E., Schmidt, W., and Bartlett, D. (2009). Characterization of the hadal microbial community in the Puerto Rico Trench and cultivation of a novel obligate psychropiezophile. ASLO Aquatic Sciences Meeting, Jan. 25-30 2009, Nice, France.
- [8] Schmidt, W., and Siegel E. (2010). On-bottom and free-fall ADCM measurements in the Puerto Rico Trench, 19.75° N, 66.40° W. Trench Connection, Nov. 10-12, 2010, Tokyo, Japan.

- [9] Hardy, K., Watson, S., and Sanderson, J. (2009). Under pressure: Testing before deployment is integral to success at sea. *Sea Technology*: 50,2. pp19-25.
- [10] Hogg, N. and Frye, D. (2007). Performance of a New Generation of Acoustic Current Meters. *J. Phys. Ocean.* DOI: 10.1175/JPO3003.1.
- [11] UNESCO (1983). Algorithms for computation of fundamental properties of seawater, 1983. UNESCO Tech. Pap. in Mar. Sci., No. 44, 53 pp.
- [12] Morgan, P. (1994). Matlab code after: Fofonoff, P. and Millard, R.C. Jr UNESCO 1983. Algorithms for computation of fundamental properties of seawater, 1983. UNESCO Tech. Pap. in Mar. Sci., No. 44, 53 pp.